A&A 551, A19 (2013)
DOI: 10.1051/0004-6361/201220281

Astronomy & Astrophysics

Attitude reconstruction for the *Gaia* spacecraft

D. Risquez[1], F. van Leeuwen[2], and A. G. A. Brown[1]

[1] Leiden Observatory, Leiden University, PO Box 9513, 2300RA Leiden, The Netherlands
e-mail: daniel.risquez@gmail.com
[2] Institute of Astronomy, University of Cambridge, Madingley Road, Cambridge, CB3 0HA, UK

Received 23 August 2012 / Accepted 23 November 2012

ABSTRACT

Context. The *Gaia* mission will produce a stereoscopic map of the Milky Way by collecting highly accurate positions, parallaxes and proper motions for about 1 billion stars. These astrometric parameters will be determined through the astrometric core solution of the *Gaia* mission which will employ about 10^8 primary sources (a subset of the observed sources with the best astrometric properties). The attitude of the spacecraft is reconstructed as part of the astrometric solution and provides the reference frame relative to which the astrometric measurements are obtained. This implies extreme demands on the accuracy of the attitude reconstruction.
Aims. This paper presents an analysis of the capabilities and limitations of the *Gaia* attitude reconstruction, focusing on the effects on the astrometry of bright ($V \lesssim 11$) stars and the implications of employing cubic B-splines in the modelling of the attitude measurements.
Methods. We simulate the attitude of the spacecraft using a realistic and very detailed model that considers not only physical effects but also technical aspects like the control system and thruster noise. We include the effect of shorter integration times for the bright stars on the effective attitude and we estimate the residual modelling noise in the reconstruction of the attitude.
Results. We provide an analysis of the dependency of the residual modelling noise in the reconstructed attitude with respect to the following parameters: integration time, B-spline knot interval, micro-propulsion system noise, and number of observations per second.
Conclusions. The final noise in the attitude reconstruction for *Gaia* is estimated to be ≈20 μas, and the main source will be the micro-propulsion system. However its effect on the astrometric performance will be limited, adding up to 7 μas rms to the parallax uncertainties. This is larger than the 4 μas from previous estimations and would affect the performance for the brightest ($V \lesssim 11$) stars.

Key words. instrumentation: miscellaneous – space vehicles: instruments – astrometry

1. Introduction

Gaia is an ESA mission dedicated to a large-scale survey of our Galaxy through astrometric, photometric and spectroscopic observations, due to be launched in 2013. *Gaia* aims at creating a 1 billion-source catalogue, complete to $V = 20$ mag, that will contain, among many other quantities, stellar parallax measurements accurate to ≃7 μas for stars at $V < 10$ mag (Lindegren et al. 2008; de Bruijne 2012).

Gaia will be a spinning spacecraft and its two telescopes will be pointing at 90° with respect to its spin axis. The spinning motion of the spacecraft is combined with a precession of the spin axis such that *Gaia*'s attitude will follow the so-called nominal scanning law (NSL). This scanning law ensures that every object is observed in at least two different scan directions during 6-month periods (de Bruijne et al. 2010). As a consequence of the spinning motion of the spacecraft the sources observed by *Gaia* will move across the CCD detectors at constant speed, and photo-electric charges will be transported at the same speed by appropriate clocking of the CCDs. This method is called time delay integration (TDI) mode. The effective integration time is the time during which electrical charges are accumulated on the detector, i.e. the time which the image of a source requires to cross the light-sensitive area of a CCD.

The spacecraft attitude is estimated on-board the spacecraft by examining the motions of stars across the focal plane. This estimated attitude is used to update the actual attitude of the spacecraft such that it keeps following the NSL. The corresponding requirement is that the absolute pointing error should be less than 1 arcmin. In the data processing on ground the spacecraft attitude is modelled as part of the astrometric solution as described in detail in Lindegren et al. (2012). In this paper we consider the limitations in the attitude reconstruction by employing a highly realistic simulation of the *Gaia* spacecraft attitude.

The main source of noise in the attitude modelling is the micro-propulsion sub-system (MPS). By MPS noise we mean the noise due to the uncertainty between the activation request and the torque finally executed by thrusters. Additional sources of noise related to the control system are its algorithms, measurements from sensors, and system delays.

The MPS thrusters provide torques along the spacecraft spin axis with an error $\sigma_\tau \approx 0.6\,\mu$Nm during 1 s time-steps (see Risquez & Keil 2010). Since the spin axis element of the inertia matrix is $I_{zz} \approx 4500\,\mathrm{kg\,m^2}$, we expect changes in the angular rate of $\dot{\omega} \approx 30\,\mu\mathrm{as\,s^{-2}}$. These changes will be applied during 1 s time-steps, and imply rotations of $\dot{\omega}\,\Delta t^2/2 \approx 15\,\mu$as with respect to a mean angular rotation. This is the order of magnitude of the angular errors that we study here.

The study presented in this paper is complementary to Lindegren et al. (2012), who extensively describe the astrometric core solution for the *Gaia* mission. The paper by Lindegren et al. (2012) made simplifying assumptions about the spacecraft attitude and in this work we use our highly realistic *Gaia* dynamical attitude model (DAM, Risquez et al. 2012) to derive insightful results regarding the possibilities and limitations of modelling the attitude of the spacecraft. The aim of this work is to analyse the angular error between the physical *Gaia* attitude and the attitude reconstruction. The paper is structured as follows. In Sect. 2 we define terms used throughout the rest of

the paper and in Sect. 3 we summarise the DAM and describe how it was used in this study. Our main results are presented in the subsequent sections. In Sect. 4 we describe the limitations in the attitude reconstruction due to the finite integration time of each observation while in Sect. 5 we describe the limitation due to the choice of modelling the attitude of the spacecraft through B-splines. In Sect. 6 we discuss a possible correction method for improving the attitude solution for bright star observations. We end with comments on the paper by Lindegren et al. (2012) in Sect. 7, and conclusions in Sect. 8.

2. Definitions

Here we define concepts related to the attitude modelling for *Gaia* and the corresponding nomenclature which is used throughout the rest of the paper.

G-band magnitude: in this paper the *Gaia G*-band magnitude is used which refers to the apparent magnitude of the sources as observed with the astrometric instrument on-board *Gaia*. As described in Jordi et al. (2010) it is a broad-band filter (FWHM 440 nm) centred on the visible part of the electromagnetic spectrum (mean wavelength 673 nm).

Directions in the fields of view: directions in the *Gaia* telescopes' fields of view are referred to as AL or AC. AL stands for *ALong scan* and refers to the direction along the great circles scanned by the telescopes as *Gaia* spins around its axis. The AL motion of stars in *Gaia*'s focal plane reflects the instantaneous spin rate of the spacecraft. AC stands for *ACross scan* and refers to the direction perpendicular to AL. The AC motion of stars in *Gaia*'s focal plane depends on the field of view. See Lindegren et al. (2012), specifically their Fig. 3, for more details.

Attitude terminology: we consider the following definitions related to the attitude:

- The *physical* attitude (also known as *true* attitude) is the attitude of the spacecraft as derived from the equations of motion and the forces acting on the spacecraft.
- The *effective* attitude is the physical attitude averaged over a certain integration time, which for bright stars depends on the CCD gate activated (cf. Sect. 3.3).
- The *astrometric* attitude is the physical attitude averaged over 4.4 s (the time required for a source to cross the full CCD). It is the reference for the mission, because it is the effective attitude seen by the astrometric instrument of *Gaia* (Bastian & Biermann 2005).
- The *demanded* attitude is the NSL, the attitude that the on-board control system is commanded to follow.
- The *on-board estimated* attitude refers to the attitude determined by the on-board control system based on measurements from the attitude sensors.

Residual modelling noise: the limitations on the attitude modelling are studied in this work by directly examining the attitude quaternions that result from the simulations of *Gaia*'s attitude with the DAM (Risquez et al. 2012). The various versions of the attitude are fitted by functions and the residual modelling noise (RMN) refers to the quality of these fits. It is the standard deviation of the differences between the attitude quaternions and the best fit model.

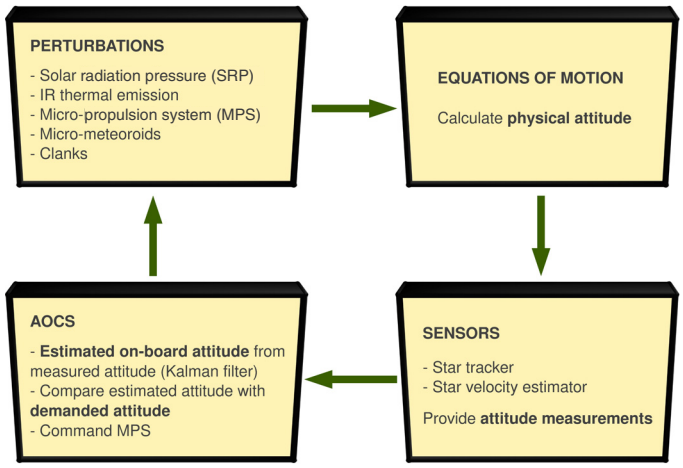

Fig. 1. General structure of the DAM. Perturbing torques (solar radiation pressure, etc.) are added up and the resulting total torque is input to the equations of motion that describe the physical attitude. The AOCS estimates the attitude using dedicated sensors and then commands the thrusters in order to follow the demanded attitude. This cycle is repeated until the simulation stops. Outputs of the simulation are the physical, astrometric and on-board estimated attitudes, and the commands sent to the MPS.

Reference systems: there are two important reference systems related to the DAM which are referred to in this paper:

- The scanning reference system (SRS) is rigidly connected to the body of the *Gaia* spacecraft (which in fact is assumed to be a rigid body). The origin of the system is *Gaia*'s centre of mass (Bastian 2007).
- The international celestial reference system (ICRS), the origin of which is located at the barycentre of the solar system and is fixed with respect to distant quasars (Feissel & Mignard 1998). The transformation between SRS and ICRS is provided by the instantaneous attitude quaternion, the output of the DAM[1].

3. Procedure

This section describes the procedure followed to estimate the attitude noise resulting from using observations with different integration times (Sect. 4), and the RMN associated with the reconstruction of the attitude (Sect. 5) from the observations.

3.1. Simulation

The physical attitude of *Gaia* is simulated using the DAM. This model simulates known perturbations to the spacecraft attitude (for instance the solar radiation pressure), hardware performances (star tracker, thrusters, etc.) and the attitude estimation algorithms implemented in the attitude and orbit control system (AOCS). A general diagram of the structure of the DAM is shown in Fig. 1. For a detailed description and example results from simulation runs refer to Risquez et al. (2011, 2012).

[1] The SRS and ICRS have different origins (spacecraft and solar-system barycentre) and are moving relative to each other, which means that the transformation between them involves more than the attitude. Strictly speaking, the relevant celestial reference system is the Centre of Mass Reference System, CoMRS (co-moving with *Gaia*), but for the purposes of this paper it is possible to ignore the difference between ICRS and CoMRS.

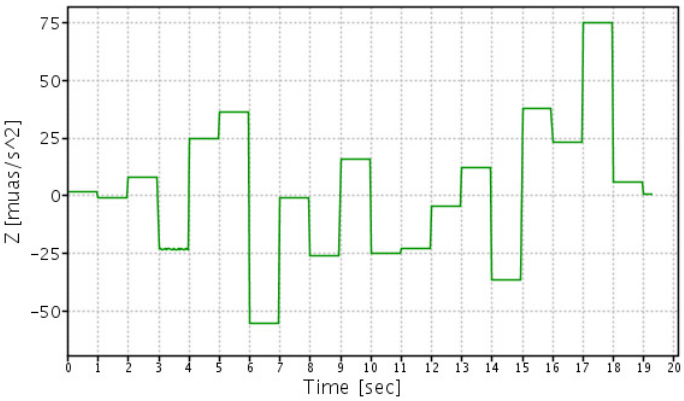

Fig. 2. Net angular acceleration around the Z axis in the SRS (i.e. AL). Accelerations around X and Y axes are similar, but with higher dispersion. Note that the simulation time-step is 0.05 s, therefore the 1 s stair-like profiles are real and reflect the AOCS loop running at 1 Hz (the AOCS commands thrusters at 1 Hz, and the thrusters work continuously).

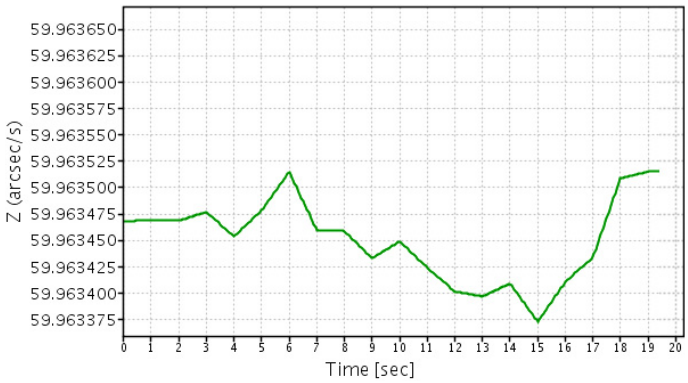

Fig. 3. Angular rates around the Z axis in the SRS (i.e. AL). The X and Y components are similar. The separation between two consecutive horizontal lines of the grid is 25 μas s^{-1}. All curves are composed of 1 s straight line segments. This is a consequence of the almost constant angular accelerations during 1 s intervals (see Fig. 2).

The DAM implements the AOCS algorithms and the on-board data streams according to specifications by the *Gaia* prime contractor EADS-Astrium. The noise levels and time delays associated with the various sensors and the MPS are also included. The main characteristics of the simulations analysed in this document are:

- Solar radiation pressure is included (see Risquez et al. 2012, for a general description).
- The MPS is modelled according to information provided by EADS-Astrium (see Risquez et al. 2012; Risquez & Keil 2010).
- Sensors: the star trackers (Risquez 2010a) and the sensor implemented by combining the detection and confirmation of sources (Risquez et al. 2012; Risquez 2010b) are simulated following EADS-Astrium documentation.
- Duration of the simulation: one spacecraft spin period, 6 h (note that the code is not limited in time and can run longer simulations).
- Time-steps in the simulation: The time-step related to the physical loop which generates the physical attitude is 0.05 s. The equations of motion are integrated numerically using this time step. The time-step related to the AOCS is 1.0 s (the AOCS works at 1 Hz), so thruster commands are updated once per second, and their torques are thus constant during one second time intervals. This is nicely seen in Figs. 2 and 3.

The state of the spacecraft is defined by an array of 7 elements, composed of the attitude (described by a quaternion, a quadruple of real numbers) and the angular rate (a 3-dimensional vector). The attitude quaternion defines the pointing direction of the spacecraft, i.e. the orientation of the SRS with respect to the ICRS. Geometrically, a quaternion defines an axis in 3-dimensional space and the angle of rotation around that axis. A summary of quaternions and their properties is provided in Appendix A of Lindegren et al. (2012).

Figure 2 presents the net AL angular accelerations (note that the orbit of *Gaia* around L2 is not simulated here). The profiles are a combination of the thrusts delivered by the MPS (commanded at 1 Hz) and the net solar radiation pressure (a sinusoidal pattern with a 6-h period). Note that the accelerations are always close to zero. Deviations from zero are due to the limited accuracy of the AOCS attitude estimates and the noise on the thrusts delivered by the MPS.

Figure 3 presents the angular rates about the spacecraft Z axis. The angular rate is larger about the Z axis (this component is about 60 arcsec s^{-1}, while the X and Y components are $<$0.2 arcsec s^{-1}).

3.2. Astrometric attitude

An image of a source observed by *Gaia* as read out from the CCD represents the average of the instantaneous source images (which move across the instrument due to the spacecraft's scanning motion) over the integration time (Bastian & Biermann 2005). From these images we can only derive the so-called astrometric attitude which roughly speaking represents the physical attitude averaged over the integration time. As explained in Bastian & Biermann (2005) the astrometric attitude is the only attitude we can reconstruct; the physical attitude is not observable.

The effective attitude we observe is thus the average of the physical attitude over an integration time interval. Mathematically this is represented by:

$$\boldsymbol{q}_{\mathrm{effective}}(\Delta t) = \left\langle \frac{\int_{t_c-\Delta t/2}^{t_c+\Delta t/2} \boldsymbol{q}_{\mathrm{physical}}(t')\,\mathrm{d}t'}{\Delta t} \right\rangle , \tag{1}$$

where $\boldsymbol{q}_{\mathrm{effective}}(\Delta t)$ is the average of the physical attitude $\boldsymbol{q}_{\mathrm{physical}}(t)$ at time t_c (centre of the integration), and Δt is the integration time.

In practice, we work with discrete data (time-steps of 0.05 s) and therefore we calculate a running average of $N = \Delta t/(0.05\,\mathrm{s})$ successive data points, referred to the mean time of these points.

Note that both Eq. (1) and the running average require quaternion re-normalisation after applying the equations because their unit length is not conserved. We indicate this re-normalisation of the quaternion components in Eq. (1) with the notation $\langle\rangle$.

3.3. Gates

In order to avoid bright stars saturating the CCDs, so-called TDI-gates may be activated, which effectively reduce the integration time for a bright source. This is achieved by draining away the charge accumulated up to the CCD column where the gate is located (see de Bruijne 2012).

Table 1. Effective integration times (second column), and RMN with respect to the physical and astrometric attitude (fourth and fifth columns); for a CCD including the effect of TDI-gate activations.

Gate number	Integration time Δt (s)	G (mag)	RMN wrt physical attitude (μas)	RMN wrt astrometric attitude (μas)
1	2.0×10^{-3}	–	–	–
2	3.9×10^{-3}	–	–	–
3	7.9×10^{-3}	–	–	–
4	1.6×10^{-2}	$-\infty$–8.84	–	–
5	3.1×10^{-2}	–	–	–
6	6.3×10^{-2}	–	–	–
7	0.13	–	–	–
8	0.25	8.84–9.59	0.063	12.6
9	0.50	9.59–10.34	0.30	12.4
10	1.01	10.34–11.10	1.05	11.8
11	2.01	11.10–11.47	3.6	9.4
12	2.85	11.47–11.95	6.2	6.7
Full CCD	4.42	11.95–∞	12.7	–

Notes. The three first columns are taken from the *Gaia* parameter database (Perryman et al. 2008). RMN with respect to the physical attitude is explained in Sect. 4.1, and with respect to the astrometric attitude is Sect. 4.2.

Table 1 shows the integration times corresponding to the gates implemented on the *Gaia* CCDs. The table also lists the range of magnitudes to which each gate applies. Note that we only consider the five longest integration times (and additionally the full CCD), and we ignore gate #4 (integration time 0.016 s) because the corresponding integration time is at least an order of magnitude shorter than the other integration times. Compared to the other gates, the effective attitude when gate #4 is activated is equivalent to the physical attitude.

3.4. Representing the time dependence of the attitude with B-splines

So far we have considered the representation of the instantaneous attitude in terms of quaternions, where the effective attitude that can be derived from *Gaia* observations represents the physical attitude convolved with (averaged over) the CCD integration time. The time dependence of the quaternion components describes the evolution of the spacecraft attitude. As described in Lindegren et al. (2012), within the astrometric global iterative solution (AGIS, the software that will provide the astrometric core solution for *Gaia*) the time dependence of the quaternion components is mathematically represented by B-splines. B-splines are piecewise functions defined in our case on a time interval. This time interval is divided into sub-intervals by means of *knots*. In AGIS, 4th order B-splines are used (i.e. piecewise cubic polynomials). B-spline functions are continuous, at knots the value from the left and from the right are the same. Analogous conditions are implemented for their first and second derivatives (continuous rates and accelerations).

The most important parameter regarding the attitude reconstruction is the length of the time interval between the knots. Shorter time intervals in principle allow for a better reconstruction of the attitude, but more parameters have to be fit to the data while there are fewer data points to support the fit. The aim of Sect. 5 is to find a trade-off between both effects.

Quaternions are normalised which means only 3 of their components are free and the fourth one is fixed by normalisation. However we fit all four components using independent B-splines. The quaternions obtained from the fitted B-splines are thus re-normalised in order to avoid any small mis-alignments.

3.5. Error angles

In this paper we will be examining the small differences between the physical attitude and the astrometric attitude or between the effective attitude and the astrometric attitude for different integration times. These attitude differences in fact represent the small differences in the orientations of two almost co-aligned spacecraft reference systems, S_1 and S_2, with respect to the ICRS, where the orientations are represented by the quaternions $\boldsymbol{q}_1$ and $\boldsymbol{q}_2$. As explained in Appendix A.6 in Lindegren et al. (2012), the orientation differences can be expressed as three small angles ϕ_x, ϕ_y, ϕ_z, which represent rotations about the axes in either S_1 or S_2. We refer to these angles as the *error angles*. When two quaternions are close, and therefore $|\boldsymbol{\phi}| \ll 1$ rad, we can calculate the angles using the following equations (Lindegren et al. 2012; Wie 1998):

$$\boldsymbol{d} \equiv \{\mathrm{d_x}, \mathrm{d_y}, \mathrm{d_z}, \mathrm{d_w}\} = \boldsymbol{q}_1^* \, \boldsymbol{q}_2, \tag{2}$$

and

$$\phi_\mathrm{x} \simeq 2\mathrm{d_x d_w}, \; \phi_\mathrm{y} \simeq 2\mathrm{d_y d_w}, \; \phi_\mathrm{z} \simeq 2\mathrm{d_z d_w}, \tag{3}$$

where $\boldsymbol{d}$ is the quaternion error (representing a frame rotation from S_1 to S_2), $\boldsymbol{q}^*$ indicates the quaternion conjugate, and $\boldsymbol{\phi} = \{\phi_\mathrm{x}, \phi_\mathrm{y}, \phi_\mathrm{z}\}$ is the 3-dimensional error angle.

The only relevant component for the astrometry is ϕ_z, the AL component. In fact, *Gaia* could be defined as a one dimensional instrument, because X and Y axes are of secondary importance. For convenience, hereafter any reference to the error angle $\boldsymbol{\phi}$ will refer implicitly to its Z component, ϕ_z.

4. Limitations related to gate activation

As described above, for very bright stars the integration time at each observation will be reduced through the activation of TDI gates. This means that for the bright stars the effective attitude is different (due to averaging the physical attitude over a shorter time interval) from that measured for the bulk of the stars. This effect can manifest itself in two ways. On the one hand when including the bright stars in the modelling of the spacecraft attitude one is mixing different effective attitudes. On the other hand when using the astrometric attitude in the solution for the astrometric parameters of bright stars one is not using the correct attitude (as "seen" by the bright stars). Both effects will lead to additional noise in the astrometric parameters derived for bright stars which reflects the attitude modelling noise.

In this section we quantify this effect by convolving the physical attitude obtained from the DAM simulations with the various integration times represented by the different gates. The result is a collection of time series of quaternions representing the attitude measured for different integration times. The distribution of the error angles between these attitude quaternions and the physical or astrometric attitude is a measure of the additional attitude modelling noise due to gate activations.

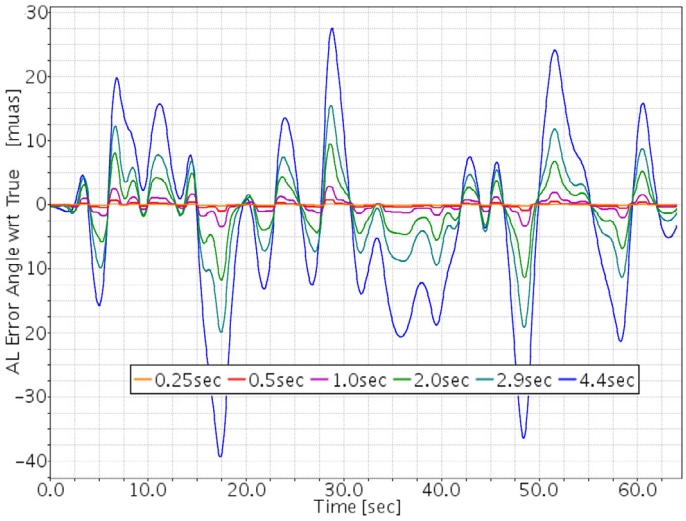

Fig. 4. Residual error angle ϕ_z (i.e. the error angle in the AL coordinate) between the physical attitude and some effective attitudes. The effective attitude depends on the activated gate. Different gates correspond to different integration times, and therefore to different average attitudes. The longer the integration time the larger the residual angle, because for longer integration times high frequency components are not captured in the effective attitude.

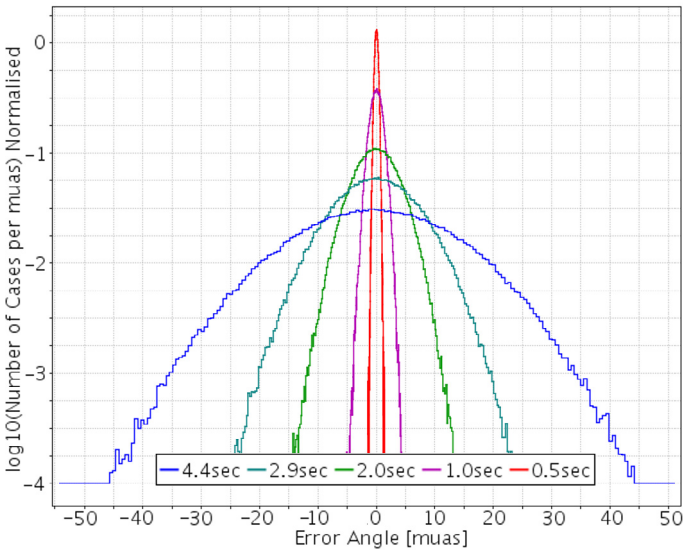

Fig. 5. Distribution of error angles (ϕ_z, effective attitude from gated observations with respect to the physical attitude). The vertical scale is logarithmic. Note that the shorter the integration time, the closer the effective attitude is to the physical attitude.

4.1. Measured attitude with respect to the physical attitude

For a short time interval Fig. 4 presents examples of the angular distance in the AL direction between the effective attitude for a given integration time (a particular gate) and the physical attitude. The longer the integration time the smoother the curve, because high-frequency components (shorter than the gate-dependent integration time) are averaged. This effect introduces a systematic difference in the attitude reconstruction when we compare attitude measurements from bright stars (gated observations) with faint stars (observed using the full CCD).

The histograms in Fig. 5 show the distribution of the error angles with respect to the physical attitude. The distributions are centred on zero (there is no systematic error) and the longer the integration time the wider the distribution. The error angle distributions are Gaussian. Table 1 presents the standard deviations of these distributions (fourth column). Empirically, these values increase approximately with the square of the integration time. This is shown in Fig. 6.

An empirical relationship can be calculated for the RMN as a function of integration time. We consider a Taylor series in the AL instrument physical attitude (ψ_i following nomenclature from Bastian & Biermann (2005), but for simplicity $\psi = \psi_i$) around the central integration time (t_c, the effective time of the observation). Note that we only consider one of the component of the attitude, the AL or equivalently the Z axis, because it is the important component for *Gaia*. Hereafter we only work with Z and ignore X and Y components, therefore ψ is always $\psi = \psi_z$.

$$\psi(t) = \psi(t_c) + \left.\frac{d\psi}{dt}\right|_{t_c}(t-t_c) + \frac{1}{2}\left.\frac{d^2\psi}{dt^2}\right|_{t_c}(t-t_c)^2 + \frac{1}{6}\left.\frac{d^3\psi}{dt^3}\right|_{t_c}(t-t_c)^3 + O\left[(t-t_c)^4\right], \quad (4)$$

where t_c is the central time of the integration and $O[(t-t_c)^4]$ indicates that the next term is proportional to $(t-t_c)^4$. In principle, high order terms (cubic and following) should be negligible, because torques are applied as second order derivatives. However,

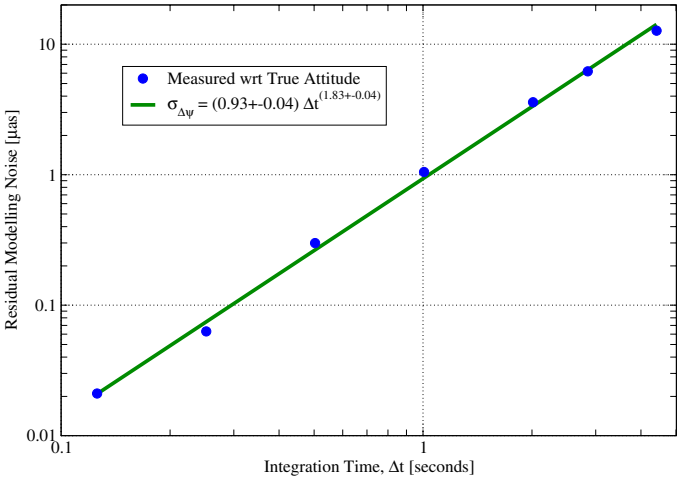

Fig. 6. Standard deviation of the error angle between the effective attitude measured during a certain integration time and the physical attitude as a function of integration time. 6 h of simulation data were processed. This data is shown in Table 1. The residual error should increase approximately with the square of the integration time, according to Eq. (7). The actual power-law slope equals 1.83 ± 0.04.

the second quaternion derivative is discrete and not differentiable when thrusters are commanded (once per second). Hence Eq. (4) is only strictly valid when $t - t_c \ll 1$ s, but it can still be used in a statistical sense as follows. We calculate the average of Eq. (4) from $t_c - \Delta t/2$ to $t_c + \Delta t/2$, and we get an approximation of the residual error as a function of the integration time:

$$\Delta\psi = \bar{\psi}_{\Delta t,t_c} - \psi(t_c) = \frac{1}{24}\left.\frac{d^2\psi}{dt^2}\right|_{t_c}\Delta t^2 + O\left(\Delta t^4\right), \quad (5)$$

where $\Delta\psi$ is the angle between the effective attitude from the gated observation and the physical attitude of the instrument, and Δt is the integration time (4.4 s in case of the full CCD).

Equation (5) is applicable to every single instant t_c, so $\Delta\psi$ are instantaneous values. From a large number of these values

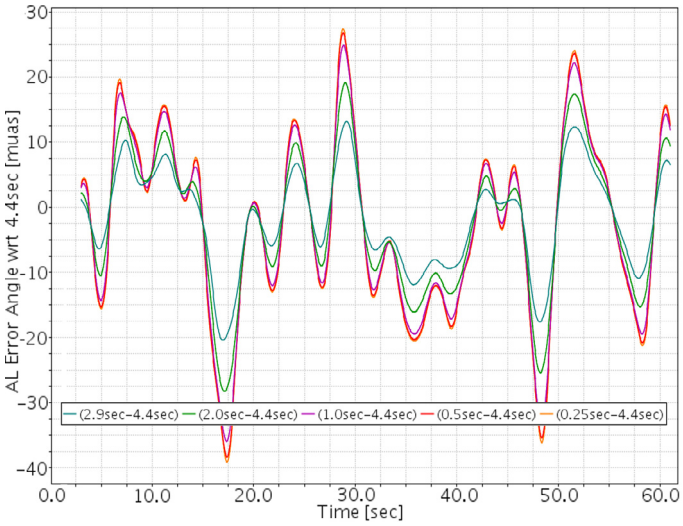

Fig. 7. Error angle in the AL direction of the effective attitude for a certain TDI gate with respect to the astrometric attitude. The effective attitude depends on the activated gate: the shorter the integration time, the larger the error angle.

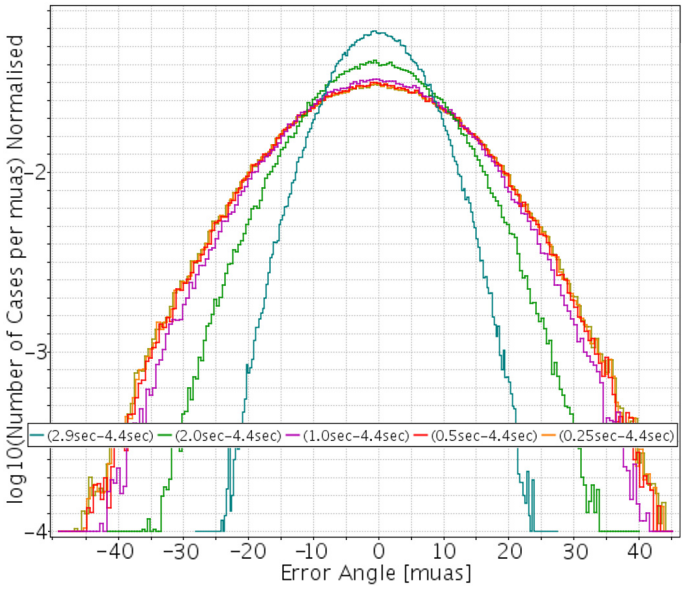

Fig. 8. Distribution of error angles ϕ_z of the effective attitude with respect to the astrometric attitude. The vertical scale is logarithmic. Note that the longer the integration time, the smaller the difference is with respect to the astrometric attitude.

we can then calculate the the variance of $\Delta\psi$:

$$\sigma^2_{\Delta\psi} = E\left(\Delta\psi^2\right) - \left[E\left(\Delta\psi\right)\right]^2, \tag{6}$$

where upon substituting Eq. (5) we get

$$\sigma_{\Delta\psi} = \frac{1}{24}\sigma_{\ddot{\psi}}\,\Delta t^2, \tag{7}$$

where

$$\ddot{\psi} = \frac{\mathrm{d}^2\psi}{\mathrm{d}t^2}. \tag{8}$$

We use the data in Table 1 to check whether statistically Eq. (5) holds over long times (i.e. one spin period). Figure 6 shows the relation between σ_{Δ_ψ} and Δt together with a linear fit to the data points. The fit is given by:

$$\sigma_{\Delta\psi} \simeq (0.93 \pm 0.04)\,\Delta t^{1.83\pm0.04}. \tag{9}$$

The empirically derived exponent of the power-law in Eq. (9) is statistically different from two, from Eq. (7), but this could be due to the simplified approximations applied to obtain Eq. (7).

We now calculate the value of the second derivative of the physical AL coordinate ($\sigma_{\ddot{\psi}}$) by using Eq. (9). From $\sigma_{\ddot{\psi}}/24 \approx 0.93$ we get $\sigma_{\ddot{\psi}} \approx 22\ \mu\mathrm{as\ s}^{-2}$. This value is an estimation of the AL noise in the attitude due to the control system and is of the same order of magnitude of the value calculated in the introduction (approx. $30\ \mu\mathrm{as\ s}^{-2}$), and similar to variations in the angular accelerations shown in Fig. 2.

In their Eq. (D.6) Lindegren et al. (2012) use a similar approach to estimate the effects of the finite CCD integration time and attitude irregularities on the interpretation of astrometric measurements for *Gaia*. Their equation is a more rigorous version of Eq. (4). We have for simplicity considered the instrument physical attitude $\psi = \psi_\mathrm{i}$ instead of the observed location of the image centre in the pixel stream.

4.2. Measured attitude with respect to the astrometric attitude

We now examine the difference between the astrometric attitude (the 4.4 s averaged physical attitude), which will be the reference attitude for the *Gaia* data processing, and the effective attitude as measured with different integration times corresponding to the gates activated for bright stars.

Figure 7 shows an example over a short time interval of the error angle of gated attitude measurements with respect to the astrometric attitude. The error angles for the shorter integration times are larger because shorter integrations are closer approximations to the physical attitude.

Figure 8 shows the distributions of the error angles. In each case the distribution is Gaussian with a standard deviation as given in Table 1 (last column). Standard deviations range from 6.7 μas for the longest gate (2.9 s) to 12.6 μas for the shortest gate (0.25 s).

Since shorter integration times provide measurements closer to the physical attitude, the last value from Table 1 and the first from the third column are almost the same. This is a remarkable result from this analysis: the difference between the attitude seen with the gated observations and the astrometric attitude corresponds to a standard deviation in the error angles of at most 12.7 μas.

Considering that the AL pixel size is 59 mas, 12.7 μas is at least 4000 times smaller. Note that the AL residual noise of a single observation of a bright star ($G \leq 13$ mag) is 92 μas (Lindegren et al. 2012), 7 times larger than the maximum noise due to gated observations. This residual noise could decrease after correcting for the quadratic term (see Sect. 6).

5. Limitations related to the B-spline representation of the attitude parameters

As explained in Sect. 3.4 the AGIS system will solve for the *Gaia* attitude parameters which are the quaternion components of which the time dependence is represented by B-splines. This

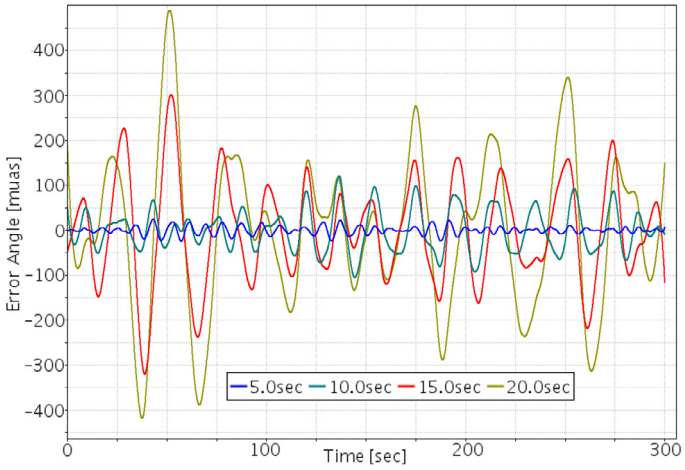

Fig. 9. AL error angle when fitting B-splines to the astrometric attitude (the physical attitude averaged over 4.4 s). Each colour indicates a different time interval between B-spline knots. This figure illustrates what we want to achieve in the attitude reconstruction: to choose the knot interval that minimises the noise due to the B-spline fit. The shorter the knot interval the smaller the amplitude of the oscillations.

is described by Eq. (10) in Lindegren et al. (2012) which we repeat here for convenience:

$$\boldsymbol{q}(t) = \left\langle \sum_{n=\ell-M+1}^{\ell} \boldsymbol{a}_n B_n(t) \right\rangle, \tag{10}$$

where the $\boldsymbol{a}_n$ are the coefficients of the B-splines $B_n(t)$ of order M (degree $M-1$) defined on the knot sequence $\{\tau_k\}_{k=0}^{N+M-1}$. The angled brackets indicate normalisation. As explained in Lindegren et al. (2012) the coefficients $\boldsymbol{a}_n$ are solved for in the attitude update step of AGIS and the solution involves the astrometric data (basically the source observation times). Here we are interested in the fundamental limitations imposed in representing the time evolution of the coefficients $\boldsymbol{a}_n$ with B-splines. Hence we do not use the astrometric observations to derive the coefficients but we *directly* fit the time sequence of components of the astrometric attitude quaternions with B-splines (i.e. we use the equation above). The quaternions we fit are obtained from the physical attitude as simulated with the DAM and convolved with the integration time corresponding to the TDI gate which was active.

The order of the B-splines is fixed to $M = 4$ in Lindegren et al. (2012) and we use the same value here (so cubic B-splines are used). However the time interval between the B-spline knots is varied in order to study the effects on the residual noise in the attitude representation.

It is important to point out here a relevant result from Holl et al. (2012), from its Appendix D. The *Gaia* attitude has four degrees of freedom per knot interval, because there are four cubic B-spline fits (one per quaternion component). However, the physical attitude only has three degrees of freedom, because quaternions are normalised. In the attitude updating of AGIS, this mismatch is managed by the attitude regularisation parameter. This parameter enforces stiffer attitude solutions, towards three degrees of freedom per knot interval. Regarding this paper, this means that AGIS will require longer time intervals to provide the same number of degrees of freedom, and we could foresee that optimum knot intervals will be longer when processing real data than in this work.

As in Sect. 4 we have again fitted 6 h worth of attitude data obtained from the DAM. Figure 9 presents some examples of B-spline fits to the astrometric attitude data. The aim of the attitude reconstruction is to recover the astrometric attitude, and therefore the best case would be a horizontal line at 0.0 μas. The error angle values oscillate as a function of time, with the amplitude of the oscillations increasing with the length of the knot interval.

Note that Fig. 9 represents the best case as we assume we know the astrometric attitude without error, which is not realistic. There are no additional sources of noise (for instance micrometeoroid impacts, noise from the thrusters), and we do not take into account the number of stars observed per unit time nor the observational errors in the astrometric data. We include the effects of the noise from the micro propulsion subsystem, astrometric measurement errors, and the number of stars in the next section.

5.1. Characterisation of the residual noise in the attitude reconstruction

In order to analyse the relation between the knot interval for the B-splines and the residual attitude modelling noise we proceed as follows:

1. The physical attitude is simulated with the DAM and then averaged over 4.4 s windows in order to obtain the astrometric attitude. The attitude simulation includes the noise associated with the MPS.
2. We simulate the effect of measurement errors in the astrometric data by generating perturbed attitude quaternions from the astrometric attitude quaternions. The perturbations are applied as small rotations around the spacecraft spin axis. These rotations simulate errors in the AL location of the sources used in the astrometric solution. The distribution of the perturbations is Gaussian with a fixed standard deviation. The observations of individual stars are simulated by generating for each time interval a number of perturbed quaternions corresponding to the expected number of observations per second.
3. We fit different B-splines (with different knot intervals) to the perturbed attitude quaternions.
4. We compute the RMN by comparing the fitted perturbed attitude and the error-free astrometric attitude (by computing the standard deviation of the AL error angle).

The results of this procedure are shown in Fig. 10 which shows that there are three different regimes: for short knot intervals the statistical noise associated with the number of observations available per knot interval is predominant; at large knot intervals the noise is dominated by the inability of the smooth B-splines to follow the high frequency features in the astrometric attitude (fitting noise); at intervals between 3 and 10 s both effects are important. The knot interval that minimises the residual noise is about 4.2 s (close to the CCD integration time), with the associated minimum noise level equal to 17 μas.

We now seek to explain the shape of the curve presented in Fig. 10 by considering the contributions of both the statistical noise $\sigma^2_{\Delta\psi,\mathrm{stat}}$ and the fitting noise $\sigma^2_{\Delta\psi,\mathrm{fit}}$ to the overall RMN $\sigma^2_{\Delta\psi}$:

$$\sigma^2_{\Delta\psi} = \sigma^2_{\Delta\psi,\mathrm{stat}} + \sigma^2_{\Delta\psi,\mathrm{fit}}. \tag{11}$$

Following Lindegren et al. (2012) the $\sigma^2_{\Delta\psi,\mathrm{stat}}$ noise term can be explained in terms of the number of observations per knot interval. For *Gaia* the average number of number of astrometric measurements per second and per telescope will be 2505. Since there are two telescopes, we get 5010 s^{-1}. We assume about 10%

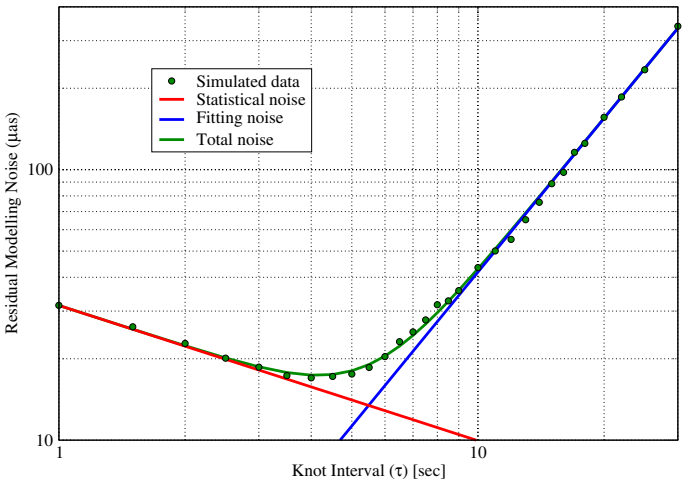

Fig. 10. RMN of the fitted perturbed attitude with respect to the error-free astrometric attitude versus the time interval between knots in the B-spline fit. The horizontal axis ranges from 1 to 30 s and the vertical axis ranges from 10 to 400 μas. The red line indicates the trend for short knot intervals (statistical noise, $\sigma_{\Delta\psi,\mathrm{stat}} \propto \tau^{-1/2}$), while the blue line indicates the trend for large knot intervals (fitting noise, $\sigma_{\Delta\psi,\mathrm{fit}} \propto \tau^{1.890\pm0.001}$). The value of the exponent is constant withing the knot intervals studied in this work. The black line is the combined noise ($\sigma_{\Delta\psi}$). The minimum noise is $\sigma_{\Delta\psi} = 17$ μas at $\tau = 4.2$ s. The noise at $\tau = 15$ s is $\sigma_{\Delta\psi,\mathrm{stat}} = 89$ μas.

of them to have good astrometric properties (not contaminated by other sources, etc.), so we take $\lambda \simeq 500$ astrometric measurements per second and we assume all of these can be used for the attitude solution.

B-splines have one degree of freedom per knot interval. If we assume that all observed stars during a time interval are combined statistically to decrease the noise in the calculation of the only one free parameter, we get

$$\sigma_{\Delta\psi,\mathrm{stat}} = \frac{\sigma_1}{N^{1/2}} = \frac{\sigma_1}{\lambda^{1/2}\tau^{1/2}} = A_{\mathrm{stat}}\tau^{-1/2}, \tag{12}$$

where

$$A_{\mathrm{stat}} = \sigma_1\,\lambda^{-1/2}, \tag{13}$$

τ is the time interval between knots, $N = \lambda\,\tau$ is the total amount of AL measurements in this interval, and σ_1 is the AL position accuracy when observing a single star (the mean value over all magnitudes is $\sigma_1 \approx 700$ μas). The statistical noise thus decreases as $\tau^{-1/2}$.

The fitting noise term reflects the inability of the B-splines to follow the high frequency features in the astrometric attitude and we can thus expect it to behave much like the variance in the difference between the astrometric (i.e. 4.4-s smoothed) and the physical attitude. The latter was approximately described by the power-law in Eq. (9). Fitting a power-law to the RMN at long knot intervals we obtain:

$$\sigma_{\Delta\psi,\mathrm{fit}} \simeq A_{\mathrm{fit}}\tau^{a_{\mathrm{fit}}}, \tag{14}$$

with the noise $\sigma_{\Delta\psi,\mathrm{fit}}$ in μas and τ in seconds. The RMN increases with the knot interval because longer knot intervals lead to B-splines that are "stiff" with respect to features in the data so that they cannot properly fit the astrometric attitude. From fitting the points at long knot interval in Fig. 10 we find $a_{\mathrm{fit}} = 1.890 \pm 0.008$. This parameter is a kind of damping factor, it indicates how much the B-splines smooth out irregular signals in the astrometric attitude.

In the next subsections we analyse in more detail the effects of the number of sources observed per knot interval, the noise from the attitude control system, and the errors in the astrometric measurements (AL location of sources).

5.2. Sources of residual noise in the attitude reconstruction

In this subsection we estimate the effect of different environments in the attitude reconstruction. We test three different sources of noise using DAM:

1. The noise in the attitude resulting from the spacecraft attitude control system, in particular the MPS. The *Gaia* spacecraft should closely follow the NSL and this is achieved through the AOCS, consisting of attitude sensors, attitude estimation algorithms, and the MPS. The AOCS will not be able to make *Gaia* follow the NSL exactly because of measurement errors in the attitude sensors, estimation errors in the algorithms that infer the attitude from the sensor data, and the noise in the execution of the micro propulsion thrust commands. This will lead to features in the astrometric attitude with characteristic times of about 10 to 100 s (seen in typical plots from the DAM), which will result in differing values of the term A_{fit}. Specifically, we simulate different noise in the force provided by thrusters (no noise at all, $\times$0.5, $\times$1.0, or $\times$2.0 their nominal values). The effect can be appreciated in the top panel of Fig. 11; there is no effect for small τ and the RMN is proportional to the MPS noise for large τ.
2. We study the effect of the number of observed stars per second on the reconstruction of the attitude. We consider *primary sources*, i.e. stars brighter than $G = 18$ mag, with no TDI gates activated, and having good astrometric properties. In this experiment, we keep the control system working in its nominal mode. The maximum and minimum number of AL measurements per second (λ) has been estimated using the *Gaia* parameter database (Perryman et al. 2008). We consider stars fainter than $G = 11.95$ mag and brighter than $G = 18$ mag, and the lines of sight of both telescopes. We get a minimum of $\lambda = 8\,\mathrm{s}^{-1}$ as a representative minimum value, and a maximum of $\lambda = 8000\,\mathrm{s}^{-1}$. See Fig. 11 (central panel) for graphic results. There is little effect for large τ, and the RMN is proportional to $\lambda^{-1/2}$ for small τ, as predicted by Eq. (12).
3. We also analyse the effect of the measurement errors in the AL location of the stars observed by *Gaia*. Ultimately the attitude is solved from the *Gaia* observations so this is an important attitude modelling noise source to consider. We follow the same procedure as before, now keeping the AOCS noise and the average number of observations per second fixed. Typically, the measurement error for a star at $G = 16$ mag is about 350 μas, at $G = 17.5$ mag the error is $\sim$700 μas, and at $G = 19$ mag the error is $\sim$ 1400 μas. In the simulations we used these three values as the mean measurement error for *all* stars. This effect is presented in Fig. 11 (bottom panel). According to the plot there is no effect for large τ, and the RMN is proportional to σ_1 for small τ, as predicted by Eq. (12).

Note that in tests #1 and #2 we assume 700 μas measurement errors for all stars.

After all these experiments, we conclude that the RMN follows closely Eq. (15), which is an elaboration on Eq. (11).

$$\sigma^2_{\Delta\psi} = \frac{\sigma_1^2}{\lambda\,\tau} + (0.53 \pm 0.01)^2 A^2_{\mathrm{MPS}}\tau^{(3.780\pm0.002)} \tag{15}$$

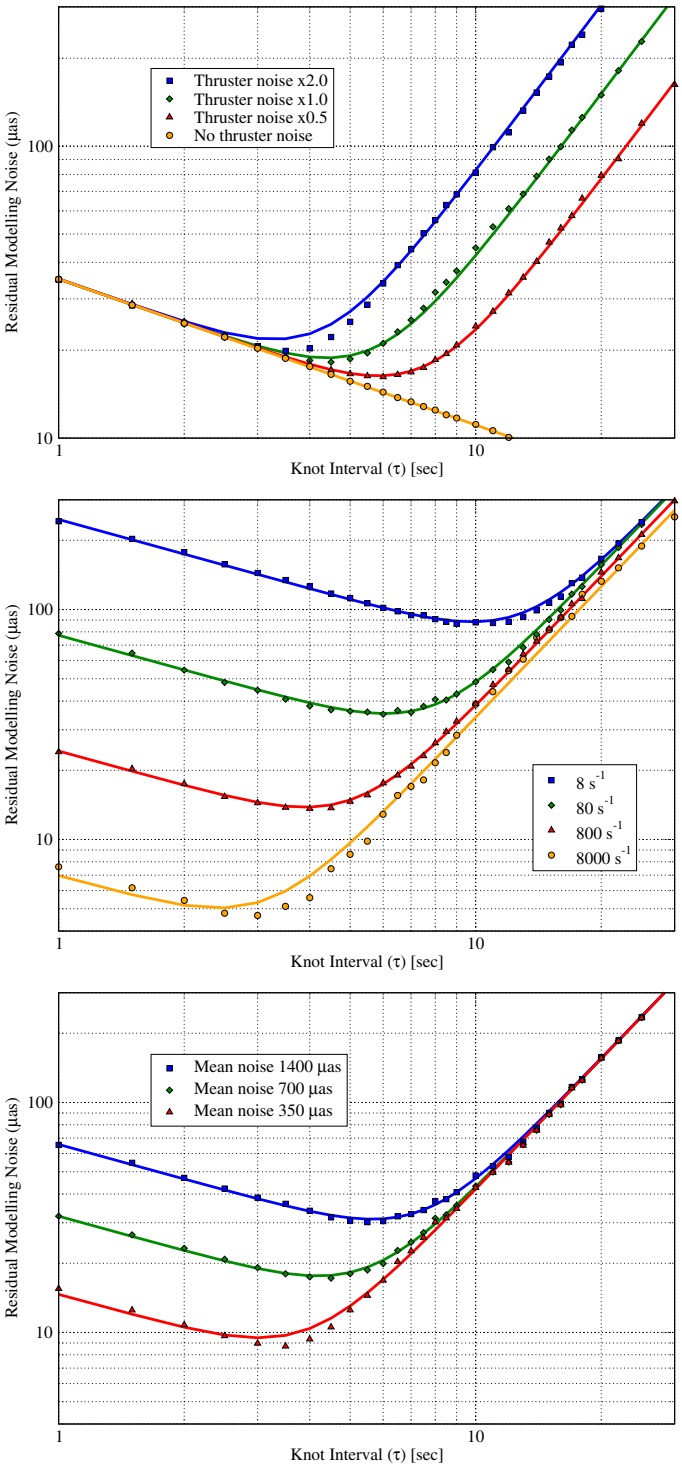

Fig. 11. RMN of the fitted perturbed attitude with respect to the error-free astrometric attitude versus the time interval between knots in the B-spline fit. Each group of symbols represents a different set of experiments per panel. The *top panel* shows the effect of different thruster noise levels (test #1 in Sect. 5.2), the *middle panel* presents the RMN with respect to different number of observations per second (see test #2), and the *bottom panel* shows the effect of different mean star magnitudes (test #3). All horizontal axes range from 1 to 30 s, and the curves represent the result of fitting Eq. (15) to the data points.

In Eq. (15), the term $A_{\rm MPS}$ represents the relative noise in the force provided by thrusters compared to their nominal values ($A_{\rm MPS}$ = 0.5, 1.0, 2.0, etc.), 0.53 is an average value, and 0.01 is an educated guess of the error after several simulations. Note that the left term depends on the number of observations per second (combined FoV) and their characteristic noise, and the right term depends on the control system (which is nominally constant during the mission).

5.3. Selection of the optimal knot interval

In this subsection we estimate what the optimal knot interval is for which the noise in the attitude reconstruction is minimised. We assume constant noise due to the MPS, equal to its expected value (case ×1.0 in Fig. 11, top panel). After differentiating Eq. (11) with respect to the knot interval (τ), we get the knot interval that provides the minimum noise ($\tau_{\rm min}$):

$$\tau_{\rm min} = \left(-\frac{A_{\rm fit}^2 a_{\rm fit}}{A_{\rm stat}^2 a_{\rm stat}} \right)^{-\frac{1}{2(a_{\rm fit}-a_{\rm stat})}}. \tag{16}$$

Typical values for the various constants are: $A_{\rm stat} = 31.47$, $A_{\rm fit} = 0.5388$, $a_{\rm fit} = 1.890$, and $a_{\rm stat} \equiv -1/2$. With the assumption of constant and nominal MPS noise we can write the optimum knot interval as a function of the statistical noise constant ($A_{\rm stat}$):

$$\tau_{\rm min} = \left(-\frac{A_{\rm fit}^2 a_{\rm fit}}{a_{\rm stat}} \right)^{-\frac{1}{2(a_{\rm fit}-a_{\rm stat})}} A_{\rm stat}^{\frac{1}{a_{\rm fit}-a_{\rm stat}}} \simeq 0.981\, A_{\rm stat}^{0.418}. \tag{17}$$

Assuming that observed stars have always a mean AL noise σ_1 = 700 μas, we re-write Eq. (17) using Eq. (13), and obtain $\tau_{\rm min}$ as a function of the number AL measurements.

$$\tau_{\rm min} = \left(-\frac{A_{\rm fit}^2 a_{\rm fit}}{a_{\rm stat}\sigma_1^2} \right)^{-\frac{1}{2(a_{\rm stat}-a_{\rm fit})}} \lambda^{-\frac{1}{2(a_{\rm stat}-a_{\rm fit})}} \simeq 15.2\, \lambda^{-0.209}. \tag{18}$$

The optimum knot interval is relatively insensitive to changes in the rate of measurements. A decrease in three orders of magnitude in the rate of measurements (from 8000 s^{-1} to 8 s^{-1}) increases the optimum knot interval from 2.3 s to 9.8 s (only a factor 4). The corresponding attitude RMN ranges from 5 μas (high density areas) to 90 μas (low density areas).

Interestingly (see Fig. 11, central panel, related to the number of observations per second) the maximum optimum knot interval ($\tau_{\rm min}$ = 9.8 s) is almost double the average ($\tau_{\rm min}$ = 4.2 s, when λ = 500 s^{-1}), and which is almost double the knot interval for high density areas ($\tau_{\rm min}$ = 2.3 s). We can take advantage of these facts in order to select the best knot interval. A good approach could be to implement the knot interval in three levels (2.5, 5 and 10 s, for example), depending on the number of AL measurements per second.

Using this approach, the attitude reconstruction is always performed with the best (or very close to the best) knot interval. This idea is very similar to the activation of CCD gates in order to observe each star with the best integration time.

6. Correction term to attitude measurements using gates

Lindegren et al. (2012) suggest that the third term in their Eq. (D.6), which is equivalent to the third term in our Eq. (4), might be corrected for by computing the second derivative $\ddot{\psi}$ from the astrometric attitude in order to make the bright star astrometric measurement also refer to the effective astrometric attitude. This would thus alleviate the problem that bright stars "see" a different attitude than the bulk of the stars observed by

Gaia. In this section we examine how well this correction works. Note that we do not address the issue of the "attitude lag" identified in Bastian & Biermann (2005) (i.e. the attitude seen by bright stars is not only different in terms of high frequency content but is also observed at a slight different moment in time, of order half the difference in integration time).

We take the following steps to assess whether the proposed correction of the bright star measurements is feasible, and if so, whether it provides a significant improvement:

1. Calculate the astrometric attitude from the simulated physical attitude. For the real mission the astrometric attitude is the attitude solution provided by AGIS.
2. Fit B-splines to the astrometric attitude in order to represent the reconstructed attitude. This fit depends on the knot interval and it is performed in the ideal case in which we know perfectly the astrometric attitude (we do not simulate individual observations and their errors).
3. Calculate numerically the second derivative of the quaternions from the B-spline fit. Keep in mind that ideally we should calculate the second derivative from the physical attitude in order to apply Eq. (7). In practice we only have access to the B-spline approximation to the astrometric attitude.
4. Calculate the correction using Eq. (19). Constants that multiply the second quaternion derivative are empirically estimated and applied, but their theoretical values seem to provide similar results.
5. Correct the AL coordinate ψ for the bright stars. This is equivalent in our case to correcting the attitude quaternions representing the effective attitude for the bright stars. The aim is to assess whether the RMN presented in Table 1 (last column) is indeed reduced significantly when applying the correction.

According to Eq. (5) the correction term with respect to the physical attitude is in first approximation proportional to the second derivative of the error angle ψ. Considering the correction with respect to the astrometric attitude we get:

$$\Delta\psi = \bar{\psi}_{\Delta t,t_c} - \bar{\psi}_{4.4\mathrm{sec},t_c} = -\frac{1}{24}\left(\Delta t^2_{4.4\mathrm{sec}} - \Delta t^2\right)\left.\frac{\mathrm{d}^2\psi}{\mathrm{d}t^2}\right|_{t_c}, \qquad (19)$$

where $\bar{\psi}_{\Delta t,t_c}$ is the mean AL angular position measured for a given gate, $\bar{\psi}_{4.4\mathrm{sec},t_c}$ the mean AL angular position without gate, Δt is the integration time for the gate, $\Delta t_{4.4\mathrm{sec}}$ is the full CCD integration time, and t_c the characteristic time of the observation (middle of the integration time). The second derivative is calculated from the B-spline representation of the astrometric attitude.

The problem to be analysed here is whether the B-spline fit provides an accurate measurement of the second quaternion derivative or not. Typical features in the attitude have characteristic times of a few seconds. Hence when the time interval between knots is relatively large (for instance one minute), this correction is totally useless. But what is the improvement when the time between knots is of the same order of magnitude as the characteristic time over which attitude features vary?

In this analysis the AL angular acceleration is calculated numerically. From the B-spline fit we get the first quaternion derivative at $t_c - 0.025$ s and $t_c + 0.025$ s (plus and minus half simulation time-step). Knowing the quaternion and its derivative, we calculate the angular rate (both at $t_c - 0.025$ s and $t_c + 0.025$ s). The following equation presents the transformation

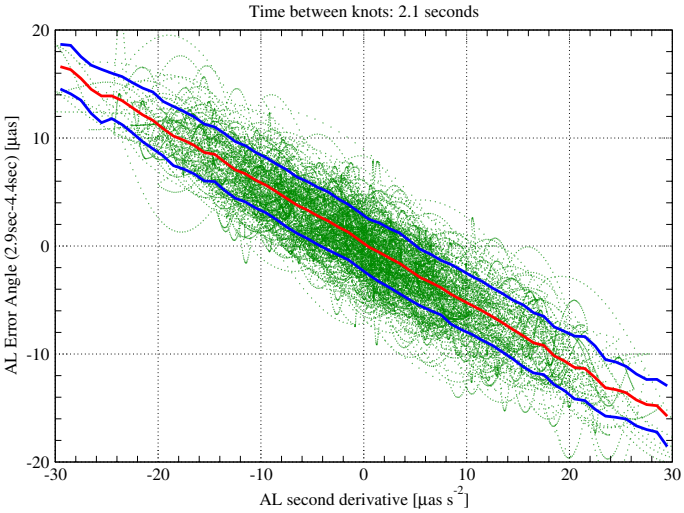

Fig. 12. $\Delta\psi$ versus $\ddot{\psi}$ as derived from the attitude data simulated with the DAM. In this case the B-spline representation of the astrometric attitude used a knot interval of 2.1 s. Each point represents a time-step (0.05 s) from the simulation. The central red line represents the mean value of the points within 1 μas s^{-2} bins, and the two adjacent blue lines are 1σ intervals (for the sake of clarity 90% of the green points are not displayed). These lines demonstrate that a linear fit is suitable. The large variance of the points around the line reflects the fact that Eq. (19) is just an approximation, valid only when the second derivative is constant during the integration time. The second derivative is actually only (approximately) constant during 1 s intervals (due to thruster commands).

from the quaternion derivative to angular rate,

$$\left\{\begin{bmatrix}\omega_x\\ \omega_y\\ \omega_z\end{bmatrix}, 0\right\} = 2\begin{bmatrix} q_4 & q_3 & -q_2 & -q_1\\ -q_3 & q_4 & q_1 & -q_2\\ q_2 & -q_1 & q_4 & -q_3\\ q_1 & q_2 & q_3 & q_4\end{bmatrix}\begin{bmatrix}\dot{q}_1\\ \dot{q}_2\\ \dot{q}_3\\ \dot{q}_4\end{bmatrix}. \qquad (20)$$

This equation is presented in Wie (1998), Eq. (5.73), and it can be worked out from of Eq. (A.18) in Lindegren et al. (2012) assuming normalised quaternions. From the angular rate difference we get the angular acceleration. Finally the AL angular acceleration is equal to $\dot{\omega}_z$, since we always work in SRS.

Figure 12 shows the results of this exercise and illustrates that indeed the relation between $\Delta\psi$ and $\ddot{\psi}$ is a linear one as expected from Eq. (19). We present the mean value in horizontal bins (red line), and the one sigma deviation band (blue lines). The distribution of residuals is Gaussian, with mean 0.0 μas and standard deviation 2.7 μas. Note that the variance around the line is rather large, suggesting that the predictive power of the proposed correction will be low.

We fitted a linear function to the data from Fig. 12. This fit is not shown in the plot, but the red line is an approximation to it. The slope of this fit is -0.55425 ± 0.00020 s^2 ($\pm 0.04\%$), its error is exceptionally small because it is the best case ($\tau = 2.1$ s).

We fitted the relation $\Delta\psi = c\ddot{\psi}$ to the data using a non-linear curve fitting (an example being shown in Fig. 12). The slopes of the fits are close to the values expected from Eq. (19). The differences are ($\approx$10%) greater than the estimated error of the slope (0.3%), and thus significant. This difference is very likely due to the control system. The AOCS implements a PID controller, i.e. Proportional, Integral and Derivative with respect to the angular distance between the on-board estimated and the demanded attitude. The proportional term is the one that we mainly observe in Fig. 12, because the applied torque (second order derivative)

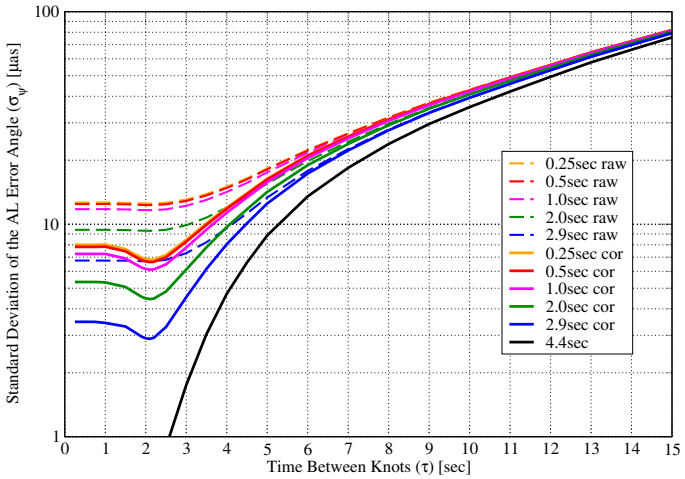

Fig. 13. RMN in the final attitude reconstruction as a function of the gate and the knot interval (considering no statistical noise due to limited observations). *raw* refers to attitude before the correction (dashed lines) and *cor* refers to corrected data (solid lines). At $\tau \simeq 2.1$ s there is a minimum in the RMN, probably related to the Nyquist-Shannon sampling theorem. The black and solid line is the reference, the RMN that we get when fitting with B-splines the astrometric attitude.

is approximately proportional to the AL error angle. The derivative (angular rate) term and the integral term contribute to the dispersion of the data, and surely changing the proportionality constant.

Figure 13 shows the results of applying the correction according to Eq. (19) to the effective attitude for sources where TDI gates were activated. It also includes the effect of the B-spline fit. The goal of the correction is to lower the discrepancy between the gated and the astrometric attitude. The solid and coloured lines show that the correction can to a limited extent indeed increase the agreement between the effective and astrometric attitude reconstructions. The results from Fig. 13 show three regimes in the correction, depending on the knot interval.

At very long B-spline knot intervals ($\gtrsim$8 s) the correction does not work at all. This is because for long knot intervals the B-spline fitting errors dominate and remove any correlation between $\ddot{\psi}$ as calculated from the astrometric attitude and the value of $\ddot{\psi}$ at the middle of the TDI gate integration time.

Toward shorter knot intervals the correction starts to have an effect because the astrometric attitude intrinsically contains some information at time scales shorter than the 4.4 s timescale (the convolution with the top-hat exposure function is not a perfect low-pass filter) and this information is then captured by the B-splines. The latter do however introduce their own smearing, being roughly limited in bandwidth to $\tau/2$. At very short knot intervals the correction still works but then starts to suffer from the intrinsic lack of high frequency information in the astrometric attitude. This explains the flat part of the curve at $\tau \lesssim 0.7$ s, which corresponds to the first zero in the Fourier space band-pass filter corresponding to the 4.4 s integration time for the astrometric attitude ($4.4/(2\pi) = 0.7$). In between the correction has its maximum effect at $\tau = 2.1$ s, which corresponds to the knot interval for which the B-spline bandwidth in Fourier space corresponds to the full CCD integration time. Thus this point represents the best match between the B-spline characteristics and the information content in the astrometric attitude.

The numerical values of the improvement in the RMN can be found in Table 2. These numbers show that only for very short knot intervals (around 5 s) we expect a significant improvement

Table 2. Difference in RMN between the reconstructed effective attitude for gated observations and the reconstructed astrometric attitude.

	Time interval between knots, τ (s)					
	5.0	10.0	20.0	5.0	10.0	20.0
	Residual modelling noise (μas)					
Gates	*Before* correction			*After* correction		
0.25–4.4	18.3	43.0	139.4	16.4	42.6	139.4
0.5–4.4	18.1	42.9	139.3	16.2	42.5	139.3
1.0–4.4	17.6	42.5	139.0	15.8	42.2	139.0
2.0–4.4	15.5	41.0	138.0	14.2	40.8	138.0
2.9–4.4	13.4	39.4	136.8	12.5	39.3	136.8

Notes. These values are corrected using the second order quaternion derivative.

(≈10%) in the RMN after applying the correction. In practice these knot intervals can only be used in the higher density regions. For the bulk of the sky longer knot intervals will be used which do not warrant applying the correction of the attitude reconstruction for gated observations.

Table 2 also shows that the improvement after the correction is small for 10-s knot intervals, and completely negligible for longer knot intervals.

7. Comments on the attitude reconstruction in Lindegren et al. (2012)

During the actual *Gaia* mission the attitude will have to be reconstructed from the astrometric measurements (source transit times). This will be done as part of the Astrometric Global Iterative Solution which is described in Lindegren et al. (2012). In their work (Lindegren et al. 2012) made some simplifications regarding both the number of sources observed and the attitude of the spacecraft:

- AGIS was applied to a subset of the expected data: about 2.3×10^6 primary sources instead of 10^8 (the latter is the expected value during the mission).
- The attitude perfectly followed the NSL, without any noise due to the MPS.
- The knot interval for the attitude reconstruction was constant all over the sky and equal to 240 s.

The converged RMN in the reconstructed attitude as determined from the AGIS run described in Lindegren et al. (2012) is $\sigma_{\Delta\psi} = 20\ \mu$as (see their Sect. 7.2.3). How does that number compare to the results found in our study?

We proceed to reproduce this value using our empirical relation (Eq. (13)). Lindegren et al. (2012) used $10^8/2.3 \times 10^6 = 43$ times less observations of primary sources than the expected number for the real *Gaia* mission, which implies $\lambda \approx 500/43 = 11.5\ \mathrm{s}^{-1}$. Inserting this value into Eq. (13), we get $A_{\mathrm{stat}} \approx 206$. The simulated spacecraft attitude in Lindegren had no noise due to the MPS, which means $A_{\mathrm{fit}} = 0$. Combining the values for A_{stat} and A_{fit} with a knot interval of $\tau = 240$ s, we get $\Delta\psi = 13\ \mu$as from Eq. (11). The same estimate was obtained by Lindegren et al. (2012) from considering the number of observations per knot interval and the weighted mean error on the AL coordinate determined for each observation. The fact that AGIS converged on an RMN of 20 μas in the reconstructed attitude can be explained by the varying sky density and the fact that the long knot interval means that the B-splines cannot perfectly represent the

NSL (see Sect. 7.2.3 in Lindegren et al. 2012). In the absence of noise in the MPS our results thus confirm the estimates by Lindegren et al. (2012). Note that for the actual *Gaia* mission Lindegren et al. (2012) estimate an attitude reconstruction RMN of 12 μas (taking into account the larger number of observations and a much shorter B-spline knot interval).

We can now make a more realistic assessment of the expected attitude reconstruction noise by using the results from our study, including the effects of the noise in the MPS. From Fig. 10 we can estimate that the minimum RMN in the attitude reconstruction will then be ~17 μas. If we allow for a 50% margin to account for a varying density of stars on the sky we get an expected noise in the reconstruction of the attitude for *Gaia* of ~26 μas. This noise could be lowered if a variable knot interval, depending on the density of stars, is used, but we do not consider this option further.

We estimate the impact of the RMN in the attitude reconstruction following Lindegren et al. (2012). As they explain, for most stars the propagation of random observational errors from individual AL observations to the parallaxes (or any other astrometric parameter) is mainly governed by geometrical factors and the total number of observations per stars. This can be statistically described by a coefficient of improvement which is estimated by Lindegren et al. (2012) to be between 0.09 and 0.27 depending on the correlation length in the attitude errors which is set by the B-Spline knot interval. We thus estimate from our work that the additional uncertainty in the parallaxes will be between about 3 and 7 μas rms. This would mainly affect the bright stars.

Our results show that, as expected, the noise in the MPS will increase the RMN in the attitude reconstruction for *Gaia*. However the effect on the astrometric performance will be limited, adding up to 7 μas rms to the parallax uncertainties. This is larger than the $\lesssim$4 μas estimated by Lindegren et al. (2012) and would affect the performance for the brightest ($V \lesssim 11$) stars.

Finally, the impact of this increase in the estimation of the attitude noise can be assessed following calculations by Lindegren et al. (2012). The total expected uncertainty in the parallax for bright stars ($G < 13$ mag) is 7.5 μas. We consider two contributions: the attitude noise (estimated in that paper to be 4 μas) and the rest of effects. Assuming that these terms can be added quadratically, we get that all non-attitude related terms equal $(7.5^2 - 4^2)^{1/2} = 6.3$ μas. On the other hand, we consider the attitude RMN from this work, up to 7 μas instead of 4 μas. Considering this higher attitude noise, the total RMN is $(6.3^2 + 7^2)^{1/2} \simeq 9$ μas. Therefore we conclude that in the best case, for the brightest stars ($G < 13$ mag), the uncertainty in the parallax will be up to 9 μas instead of 7.5 μas. Similar relations hold for positions and proper motions.

8. Conclusions

In this paper we present an analysis of the capabilities and limitations of the *Gaia* attitude reconstruction, focusing on two topics: the effect of gates in the observation of bright stars, and the use of B-splines to fit the attitude.

This analysis was performed using simulated attitude of the spacecraft from the DAM, a realistic and very detailed model. It considers the physics of the spacecraft (equations of motion, inertia matrix, etc.) and it also implements the control system (AOCS and its algorithms, sensors, thrusters). This model provides very insightful results that allows us to analyse the attitude reconstruction.

According to our results, shorter integration times (gated observations) follow closely the physical attitude, but they are farther away from the astrometric attitude (the reference for the observations). According to Table 1, the RMN due to gated observations with respect to the astrometric attitude is always 6−12 μas. Since the AL error of a single observation of a bright star ($G \leq 13$ mag) is about 92 μas (Lindegren et al. 2012), the noise due to gated observations is 7 times smaller.

The RMN due to the attitude reconstruction follows Eq. (11). There are two important terms: the first related to the statistical noise (more important for short knot intervals) and the second related to the use of B-splines to model the attitude (more important for long knot intervals).

The optimal knot interval, the one that provides the lowest noise, depends on the amount of AL observations per second (considering fixed the MPS noise). Reasonable knot intervals range from 2.3 s (for high density areas of the sky) to 9.8 s (for low density areas of the sky), nearly a factor 4. Noise ranges from 5 μas in high density areas up to 90 μas in low density areas.

According to Sect. 6, to include a correction term proportional to the second order quaternion derivative of the astrometric attitude does not improve significantly the reconstruction of the attitude. Its effect is only relevant for very short knot intervals (shorter than 10 s) and its correction is always $\leq$6 μas.

In conclusion our results show that, as expected, the noise in the MPS will increase the RMN in the attitude reconstruction for *Gaia*. However the effect on the astrometric performance will be limited, adding up to 7 μas rms to the parallax uncertainties (considering only the attitude-related term). This is larger than the 4 μas estimated by Lindegren et al. (2012) and would affect the performance for the brightest ($V \lesssim 11$ mag) stars. The total uncertainty in the parallax of the brightest stars could be 9 μas instead of 7.5 μas.

Acknowledgements. This research project has been supported by NOVA (*Nederlandse Onderzoekschool Voor Astronomie*). We thank to EADS-Astrium for very kindly providing us with the detailed information and feedback necessary for a proper implementation of the simulation, C. Blasco for providing feedback during the realisation of this work, and to the referee Dr. L. Lindegren. for his helpful and detailed suggestions.

References

Bastian, U. 2007, Reference systems, conventions and notations for Gaia, Tech. rep., Astronomisches Rechen-Institut, Heidelberg (part of ZAH, Zentrum für Astronomie, Heidelberg)
Bastian, U., & Biermann, M. 2005, A&A, 438, 745
de Bruijne, J., Siddiqui, H., Lammers, U., et al. 2010, in IAU Symp. 261, eds. S. A. Klioner, P. K. Seidelmann, & M. H. Soffel, 331
de Bruijne, J. H. J. 2012, Ap&SS, 341, 31
Feissel, M., & Mignard, F. 1998, A&A, 331, L33
Holl, B., Lindegren, L., & Hobbs, D. 2012, A&A, 543, A15
Jordi, C., Gebran, M., Carrasco, J. M., et al. 2010, A&A, 523, A48
Lindegren, L., Babusiaux, C., Bailer-Jones, C., et al. 2008, in IAU Symp. 248, eds. W. J. Jin, I. Platais, & M. A. C. Perryman, 217
Lindegren, L., Lammers, U., Hobbs, D., et al. 2012, A&A, 538, A78
Perryman, M., de Bruijne, J., & Lammers, U. 2008, Exp. Astron., 22, 143
Risquez, D. 2010a, Gaia Attitude Model. Star Tracker, Tech. rep., Leiden Observatory, GAIA-C2-TN-LEI-DRO-005
Risquez, D. 2010b, Gaia Attitude Model. Star Velocity Estimator, Tech. rep., Leiden Observatory, GAIA-C2-TN-LEI-DRO-006
Risquez, D., & Keil, R. 2010, Gaia Attitude Model. Micro-Propulsion Sub-System, Tech. rep., Leiden Observatory, GAIA-C2-TN-LEI-DRO-003
Risquez, D., Keil, R., van Leeuwen, F., & Brown, A. 2011, in EAS Publ. Ser., 45, 47
Risquez, D., van Leeuwen, F., & Brown, A. 2012, Exp. Astron., 34, 669
Wie, B. 1998, Space Vehicles, Dynamics and Control (AIAA Education Series)